Available online at www.sciencedirect.com
ScienceDirect
Applied Mathematics and Computation 200 (2008) 537–546
APPLIED MATHEMATICS AND COMPUTATION
www.elsevier.com/locate/amc

Chebyshev pseudospectral method for computing numerical solution of convection–diffusion equation

F.S.V. Bazán

Department of Mathematics, Federal University of Santa Catarina, 88040-900 Florianópolis SC, Brazil

Abstract

A method for computing highly accurate numerical solutions of 1D convection–diffusion equations is proposed. In this method, the equation is first discretized with respect to the spatial variable, transforming the original problem into a set of ordinary differential equations, and then the resulting system is integrated in time by the fourth-order Runge–Kutta method. Spatial discretization is done by using the Chebyshev pseudospectral collocation method. Before describing the method, we review a finite difference-based method by Salkuyeh [D. Khojasteh Salkuyeh, On the finite difference approximation to the convection–diffusion equation, Appl. Math. Comput. 179 (2006) 79–86], and, contrary to the proposal of the author, we show that this method is not suitable for problems involving time dependent boundary conditions, which calls for revision. Stability analysis based on pseudoeigenvalues to determine the maximum time step for the proposed method is also carried out. Superiority of the proposed method over a revised version of Salkuyeh's method is verified by numerical examples.

Keywords: Convection; Diffusion; Chebyshev pseudospectral method; Stability region; Pseudoeigenvalues

1. Introduction

We consider numerical methods for the 1D convection–diffusion equation

$$\frac{\partial u}{\partial t} + c\frac{\partial u}{\partial x} = \gamma \frac{\partial^2 u}{\partial x^2}, \quad 0 \leqslant x \leqslant 1 \tag{1}$$

subject to the initial and boundary conditions

$$\begin{aligned} &u(x,0) = f(x), \quad 0 \leqslant x \leqslant 1, \\ &u(0,t) = g_0(t), \quad t \geqslant 0, \\ &u(1,t) = g_1(t), \quad t \geqslant 0. \end{aligned} \tag{2}$$

Partial differential equations (PDEs) like these appear in connection with problems in fluid mechanics, financial mathematics, and many other fields. The numerical solution of the problem is a topic of research that

E-mail address: fermin@mtm.ufsc.br

0096-3003/$ - see front matter © 2007 Elsevier Inc. All rights reserved.
doi:10.1016/j.amc.2007.11.026

has provided a challenge of lasting interest in numerical analysis and resulted in a number of methods, see e.g. [3,6,7,9–11]. The purpose of this paper is to propose a method for solving convection–diffusion equations based on the Chebyshev pseudospectral (CPS) collocation method. This choice is supported by the excellent reputation of CPS amongst practitioners due to its high accuracy and relatively low computational cost [2,4,12,13]. For this reason, the numerical solutions of (1) and (2) by using a pseudospectral method should be highly accurate as well.

Before describing the proposed method, we review a finite difference approach (FDA) by Salkuyeh [7], and, contrary to the proposal of this author, we show that FDA does not apply when the problem involves time dependent boundary conditions, which calls for revision.

Both methods CPS and FDA start by discretizing (1) and (2) with respect to the spatial variable, transforming the problem into a system of ordinary differential equations (the semidiscrete counterpart of (1) and (2)),

$$\frac{\mathrm{d}\mathbf{V}}{\mathrm{d}t} = \mathbf{A}\mathbf{V} + \mathbf{b}(t), \quad \mathbf{V}(0) = \mathbf{V}_0, \tag{3}$$

where $\mathbf{A}$ is a matrix and $\mathbf{V}$, $\mathbf{b}$ are the vector valued functions of dimension N_h. Subscript h is a positive parameter that determines the spatial grid and all these quantities depend on the spatial discretization chosen. The numerical solution itself is then constructed in a second stage by integrating the corresponding semidiscrete system (3). Thus, the methods differ in the way the corresponding semidiscrete system is integrated in time. While the CPS method computes the solution $\mathbf{V}(t)$ by using the fourth-order Runge–Kutta method, Salkuyeh's approach computes the solution $\mathbf{V}(t)$ by using an exact formula for the exponential matrix $\exp(\mathbf{A}t)$ at a given time level t. The paper is organized as follows. In Section 2 we reintroduce the finite difference approach by Salkuyeh and show why it does not apply for problems involving time dependent boundary conditions. Comments about stability of FDA are included. The proposed pseudospectral method is described in detail in Section 3 and stability issues are discussed in Section 4. Numerical results that illustrate the efficiency of the proposed method are reported in Section 5. Section 6 contains concluding remarks.

2. Semidiscrete problem from finite differences

Perhaps the simplest way to transform problem (1)–(2) into a system of ODEs is by centered finite differences. Let $x_i = hi,\ i = 0,\ldots,m$ be a set of regular grid points of the interval $[0,1]$ with $x_0 = 0,\ x_m = 1$, and $h = 1/m$. Then it is well known that

$$\frac{\partial u}{\partial x}(x_i,t) = \frac{u(x_{i+1},t) - u(x_{i-1},t)}{2h} + \mathcal{O}(h^2),$$
$$\frac{\partial^2 u}{\partial x^2}(x_i,t) = \frac{u(x_{i+1},t) - 2u(x_i,t) + u(x_{i-1},t)}{h^2} + \mathcal{O}(h^2).$$

If we neglect the approximation error and introduce $v_i(t)$ to denote the values approximating $u(x_i,t)$, we transform (1) and (2) into a system of $m-1$ ordinary differential equations:

$$\begin{cases} \frac{\mathrm{d}\mathbf{V}}{\mathrm{d}t} = \mathbf{A}_d\mathbf{V} + \mathbf{b}(t), \\ \mathbf{V}(0) = [f(x_1),\ldots,f(x_{m-1})]^{\mathrm{T}}, \end{cases} \tag{4}$$

where

$$\mathbf{A_d} = \frac{1}{h^2}\begin{bmatrix} p & r & & & \\ q & p & r & & \\ & \ddots & \ddots & \ddots & \\ & & q & p & r \\ & & & q & p \end{bmatrix}_{(m-1)\times(m-1)}, \quad \mathbf{b}(t) = \frac{1}{h^2}\begin{bmatrix} qg_0(t) \\ 0 \\ \vdots \\ 0 \\ rg_1(t) \end{bmatrix}, \tag{5}$$

with

$$p = -2\gamma, \quad q = \gamma + \frac{ch}{2}, \quad r = \gamma - \frac{ch}{2}.$$

The solution to (4) subject to the given initial condition is readily shown to be [1]

$$\mathbf{V}(t) = \mathrm{e}^{\mathbf{A}t}\mathbf{V}(0) + \frac{1}{h^2}\left[q\int_0^t \exp(\mathbf{A}_d(t-\tau))g_0(\tau)\mathbf{e}_1\,\mathrm{d}\tau + r\int_0^t \exp(\mathbf{A}_d(t-\tau))g_1(\tau)\mathbf{e}_{m-1}\,\mathrm{d}\tau\right], \tag{6}$$

where $\exp(\mathbf{A}_d t)$ stands for the exponential of $\mathbf{A}_d t$ and $\mathbf{e}_i$ is the ith canonical vector in $\mathbb{R}^{m-1}$.

When $\mathbf{b}(t)$ does not depend on t, which is the case when the boundary conditions in (2) are constant, the unique solution to (4) reduces nicely to

$$\mathbf{V}(t) = -\mathbf{A}_d^{-1}\mathbf{b} + \exp(t\mathbf{A}_d)(\mathbf{V}(0) + \mathbf{A}^{-1}\mathbf{b}). \tag{7}$$

This $\mathbf{V}(t)$ together with an explicit formula for $\exp(t\mathbf{A_d})$ at a fixed time level t is used by Salkuyeh in [7] to compute numerical solutions of test problem of type (1)–(2) involving time dependent boundary conditions. Ignoring the fact that the numerical results reported in [7] are incorrect because (7) holds only when the boundary conditions are constant, what should be emphasized here is that $\exp(t\mathbf{A}_d)$ is easy to compute in this case because $\mathbf{A}_d$ is diagonalizable, i.e., $\mathbf{A}_d = P\Lambda P^{-1}$, and because both the eigenvector matrix P and the matrix of corresponding eigenvalues Λ are known in closed form [5]. This was exploited by Salkuyeh to determine a closed form for P^{-1} and hence for $\exp(t\mathbf{A}_d)$. Specifically, Salkuyeh uses the fact that the columns of P are of the form [5]

$$p_i = \begin{bmatrix} (q/r)^{1/2}\sin(1i\pi/m) \\ (q/r)^{2/2}\sin(2i\pi/m) \\ \vdots \\ (q/r)^{(m-1)/2}\sin((m-1)i\pi/m) \end{bmatrix}, \quad i = 1,\ldots,m-1, \tag{8}$$

and concludes in a closed form for P^{-1}. A crucial point ignored here is that because (q/r) is always larger than 1, the powers of this quotient yield ill-conditioning in P when n is large enough. Another important observation is that the left factor $1/h^2$ and the dependence of $\mathbf{b}$ on t in (5) are ignored in the paper by Salkuyeh. We wonder how this author incorporated time dependent boundary conditions into vector $\mathbf{b}$ independent of t. Anyway, since matrix $\mathbf{A}_d$ is tridiagonal Toeplitz, this property can be exploited to implement (6) in a numerically stable way, without using any explicit form for P^{-1} even if the problem involves time dependent boundary conditions. In fact, to compute stably $P^{-1}\mathbf{b}$ it suffices solving the system $Px = \mathbf{b}$ using a matrix P of normalized eigenvectors. Below we give some details of an implementation of the difference-finite-based method for the case where the initial and boundary conditions of problems (1) and (2) are defined such that the corresponding exact solution is of the form $u(x,t) = \exp(\alpha x + \beta t)$ with parameters α and β suitably chosen. Our interest is because these are the test problems used in [7] which we also use to illustrate the potential of our method to be described in the next section. The following simple result will be used.

Lemma 1. *Let* $\mathbf{A}_d$ *have a spectral decomposition* $\mathbf{A}_d = P\Lambda P^{-1}$. *Then a necessary condition for* $u(x,t) = \exp(\alpha x + \beta t)$ *to solve problem* (1) *and* (2) *is that* $g_0(t) = \exp(\beta t)$, $g_1(t) = \exp(\alpha + \beta t)$, *and* $\gamma\alpha^2 - c\alpha - \beta = 0$. *Moreover, the approximate difference-finite-based solution becomes in this case*

$$\mathbf{V}(t) = P\left[\exp(t\Lambda)w_0 + \frac{1}{h^2}((\beta I - \Lambda)^{-1}(\exp(\beta I t) - \exp(\Lambda t))w_1)\right], \tag{9}$$

where $w_0 = P^{-1}\mathbf{V}(0)$, $w_1 = P^{-1}(q\mathbf{e}_1 + \exp(\alpha)r\mathbf{e}_{m-1})$

Proof. The first part is an immediate consequence of the fact that the solution to (1) and (2) is of the form $u(x,t) = \exp(\alpha x + \beta t)$. As for Eq. (9), it results from using $\mathbf{A}_d = P\Lambda P^{-1}$ in (6) and the specified boundary conditions. □

In Section 5, we report numerical results of an implementation of FDA that relies on (9), where P contains normalized eigenvectors and w_0 and w_1 are obtained by solving linear systems instead of using the closed form for P^{-1}. Despite the fact that this implementation has better numerical properties than the one that uses the explicit formula for P^{-1}, it is worth emphasizing that except for special cases, the truncating $\mathcal{O}(h^2)$ error in this

discretization cannot be improved. Indeed if problem (1)–(2) has solution as in Lemma 1, it is easy to prove the following result concerning the truncating error $\tau_i(t)$ at (x_i, t).

Lemma 2. *Let the solution of (1) and (2) be as in Lemma 1. Then the truncating error at (x_i, t) in discretizing (1) by finite differences satisfies*

$$\tau_i(t) \approx \left(c\frac{\alpha^3 \exp(\alpha)}{6} - \gamma \frac{\alpha^4}{12} \right) h^2 \exp(\beta t). \tag{10}$$

It is clear that this discretization error becomes small when $\alpha \ll 1$ and $\beta < 0$. This will be illustrated in Section 5.

3. Pseudospectral semidiscrete model

We concentrate on a semidiscrete method obtained by discretizing (1) with respect to the spatial variable using the pseudospectral Chebyshev method. In the following the first-order $(n+1) \times (n+1)$ Chebyshev differentiation matrix associated with the collocation points

$$0 = x_0 < x_1 < \cdots < x_n = 1, \quad \text{with } x_j = \frac{1}{2}[1 - \cos(j\pi/n)], \ \ j = 0, 1, \ldots, n \tag{11}$$

will be denoted by D. Also, if d_i (resp., l_i^{T}) denotes the ith column (resp., row) vector of matrix D, we write

$$D = [d_1, \ldots, d_{n+1}] = \begin{bmatrix} l_1^{\mathrm{T}} \\ \vdots \\ l_{n+1}^{\mathrm{T}} \end{bmatrix}$$

Let D_1, D_2, and D_3 be matrices defined by

$$D_1 = [d_2, \ldots, d_n], \quad D_2 = [l_2, \ldots, l_n]^{\mathrm{T}}, \quad D_3 = E^{\mathrm{T}} D E, \tag{12}$$

with $E = [\mathbf{e}_2, \ldots, \mathbf{e}_n]$, where $\mathbf{e}_i$ is the ith column of the identity matrix of order $n+1$.

Now let us introduce the semidiscrete version of (1) and (2) obtained by discrete differencing using matrix D. Recall that if $v = [v_0, \ldots, v_n]^{\mathrm{T}}$ denotes a vector of data at positions $x_j, \ j = 0, 1, \ldots, n$, the first-order differentiation matrix D gives highly accurate approximations to $v'(x_j), v''(x_j), \ldots$, simply by taking $v'(x_j) = (Dv)_j$, $v''(x_j) = (D^2 v)_j$, and so on. Formulae for the entries of D and an m-file for its computation can be found in several references, see e.g., Trefethen [13], where the collocation points x_i are numbered from right to left and defined in $[-1, 1]$. A slight modification of a Matlab m-file by Trefethen [13] for computing D, adapted to the interval $[0, 1]$, could go as follows:

```
%% CHEBY compute D = differentiation matrix, y = Chebyshev grid%%
  function [D,y]=cheby(N)
  if N==0, D=0; x=1; return, end
  x=cos(pi*(0:N)/N)'; y=0.5*(x+1);
  c=[2; ones(N-1,1); 2].*(-1).^(0:N)';
  X=repmat(y,1,N+1);
  dX=X-X';
  Dl=(c*(1./c)')./(dX+(eye(N+1)));     % off-diagonal entries
  Dl=Dl - diag(sum(Dl'));   % diagonal entries
  y=flipud(y);              % ordering points from left to right
  D=flipud(fliplr(Dl));     % differentiation matrix
```

The accuracy of this discrete differencing operator is illustrated in Fig. 1.

Now, let us discretize problem (1)–(2) using the Chebyshev pseudospectral collocation method. In fact, for the first-order derivative we have

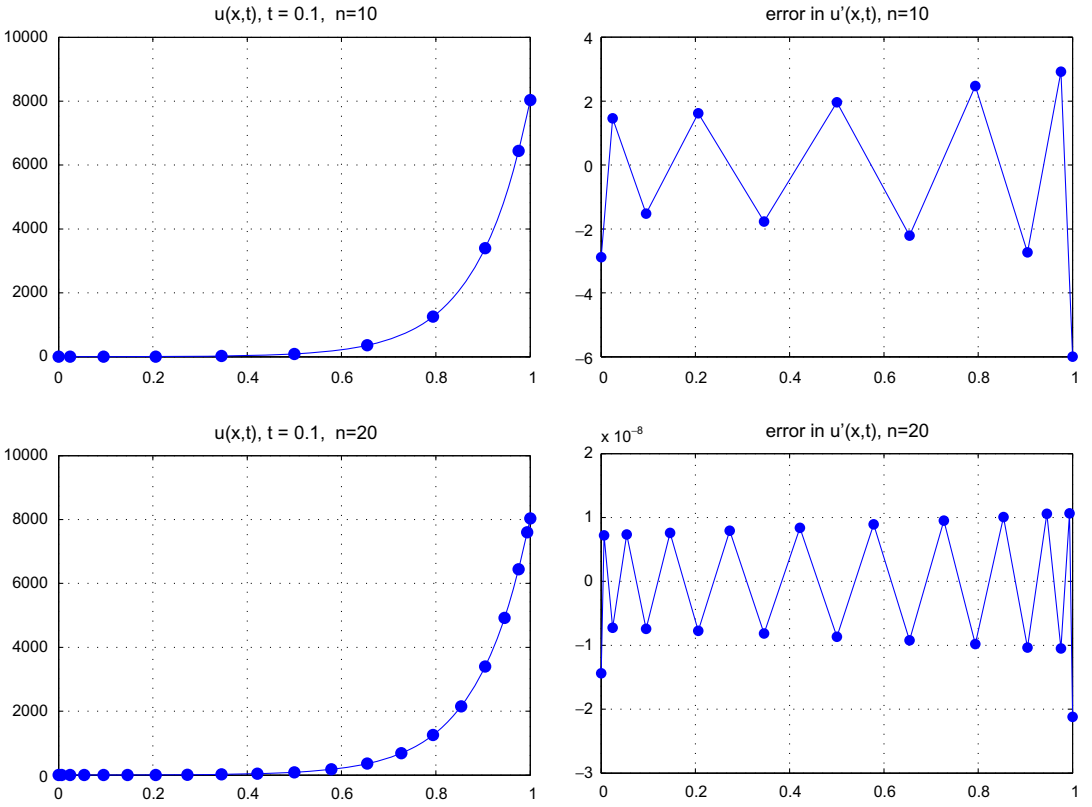

Fig. 1. Chebyshev differentiation of $u(x,t) = \exp(\alpha x + \beta t)$, with $\alpha = 9$, $\beta = -0.09$.

$$\begin{bmatrix} \frac{\partial u}{\partial x}(x_0,t) \\ \frac{\partial u}{\partial x}(x_1,t) \\ \vdots \\ \frac{\partial u}{\partial x}(x_{n-1},t) \\ \frac{\partial u}{\partial x}(x_n,t) \end{bmatrix} \approx D \begin{bmatrix} u(x_0,t) \\ u(x_1,t) \\ \vdots \\ u(x_{n-1},t) \\ u(x_n,t) \end{bmatrix} = D_1 \begin{bmatrix} u(x_1,t) \\ \vdots \\ u(x_{n-1},t) \end{bmatrix} + u(x_0,t)d_1 + u(x_n,t)d_{n+1},$$

where we have used the columnwise representation of D to deduce the last equality. Insertion of the boundary conditions shows that at interior grid points we have

$$\begin{bmatrix} \frac{\partial u}{\partial x}(x_1,t) \\ \vdots \\ \frac{\partial u}{\partial x}(x_n,t) \end{bmatrix} \approx D_3 \begin{bmatrix} u(x_1,t) \\ \vdots \\ u(x_n,t) \end{bmatrix} + g_0(t)E^T d_1 + g_1(t)E^{\mathrm{T}} d_{n+1}. \tag{13}$$

A similar procedure leads to

$$\begin{bmatrix} \frac{\partial^2 u}{\partial x^2}(x_1,t) \\ \vdots \\ \frac{\partial^2 u}{\partial x^2}(x_n,t) \end{bmatrix} \approx D_2 D_1 \begin{bmatrix} u(x_1,t) \\ \vdots \\ u(x_n,t) \end{bmatrix} + g_0(t)D_2 d_1 + g_1(t)D_2 d_{n+1}. \tag{14}$$

If we neglect the approximation error and denote by $v_i(t)$ the approximation to $u(x_i,t)$, a semidiscrete Chebyshev approximation to (1) and (2) is provided by the system of $n-1$ ODEs

$$\begin{cases} \frac{d\mathbf{V}}{dt} = \mathbf{A}\mathbf{V} + \mathbf{b}(t), \quad t \geqslant 0, \\ \mathbf{V}(0) = [f(x_1), \ldots, f(x_{n-1})]^{\mathrm{T}} \end{cases} \tag{15}$$

with x_i being defined in (11), $\mathbf{V}(t) = [v_1(t), \ldots, v_{n-1}(t)]^{\mathrm{T}}$, and

$$\mathbf{A} = \gamma D_2 D_1 - cD_3, \quad \mathbf{b}(t) = g_0(t)(\gamma D_2 - cE^{\mathrm{T}})d_1 + g_1(t)(\gamma D_2 - cE^{\mathrm{T}})d_{n+1}.$$

When a spectral decomposition of $\mathbf{A}$ is available, $\mathbf{A} = P\Lambda P^{-1}$, it is straightforward to see that the solution to the above initial value problem is

$$\mathbf{V}(t) = P\left[\exp(t\Lambda)\left(w_0 + \int_0^t \exp(-\Lambda\tau)g_0(\tau)\mathrm{d}\tau w_1 + \int_0^t \exp(-\Lambda\tau)g_0(\tau)\mathrm{d}\tau w_2\right)\right], \tag{16}$$

where $w_0 = P^{-1}\mathbf{V}(0)$, $w_1 = P^{-1}(\gamma D_2 - cE^{\mathrm{T}})d_1$, and $w_2 = P^{-1}(\gamma D_2 - cE^{\mathrm{T}})d_{n+1}$. Now if the solution of (1) and (2) is as in Lemma 1, the solution of (15) turns out to be

$$\mathbf{V}(t) = P[\exp(t\Lambda)w_0 + (\beta I - \Lambda)^{-1}(\exp(\beta It) - \exp(\Lambda t))w], \tag{17}$$

where $w_0 = P^{-1}\mathbf{V}(0)$, $w = P^{-1}(\gamma D_2 - cE^{\mathrm{T}})(d_1 + \exp(\alpha)d_{n+1})$.

Despite the fact that the eigenvalues of $\mathbf{A}$ are not known in closed form, it is worth noting that eigenvalue-based solutions for the semidiscrete system can be implemented without difficulties as long as n is a moderate number. This is so as Chebyshev differentiation matrices of moderate order, e.g., $n \leqslant 30$, very often lead to highly accurate solutions. Another possibility is using either an ODE solver for time integration or any numerical method for ODE's. The method we propose relies on this category: we regard the semidiscrete system as one of the form $\mathrm{d}\mathbf{V}/\mathrm{d}t = \mathbf{f}(t, \mathbf{V})$ and propose to integrate in time by the classical fourth-order Runge–Kutta (RK) method.

4. Stability considerations

The section is devoted to discuss the maximum stepsize for the RK method to assure stable integration for a given spatial grid. Recall that to assure stable integration of a system of ODE's with system matrix $\mathbf{A}$, close to normal, the stepsize Δt must be chosen in such a way that the spectrum of $\Delta t\mathbf{A}$ is contained in the stability region of the time integrator. Also, recall that for non-normal $\mathbf{A}$, this stability condition is not always reliable and often seen to fail when $\mathbf{A}$ is far from normal. Indeed, for such problems, the stepsize must be chosen such that the ϵ-pseudospectrum of $\Delta t\mathbf{A}$ lies within a distance $\mathcal{O}(\epsilon) + \mathcal{O}(\Delta t)$ of the stability region as $\epsilon \to 0$ and $\Delta t \to 0$ [8,13].

Thus we have to discuss whether the system matrix $\mathbf{A} = \gamma D_2 D_1 - cD_3$ in (15) is close to normal or not. To this end we first observe that while matrix $D_2 D_1$ is close to normal, this is not the case for matrix D_3 which is highly non-normal; explanation about this can be found in [12]. Since $\mathbf{A}$ combines properties of $D_2 D_1$ and D_3 in a highly non-linear way, matrix $\mathbf{A}$ should be highly non-normal as well, except probably when $c \approx 0$. This can be verified in several ways and one of these is by inspecting the ϵ-pseudospectra of $\mathbf{A}$, which is depicted in Fig. 2 for two different choices of constants c and γ and with $n = 30$. In both cases matrix $\mathbf{A}$ has a pair of "outlier" eigenvalues at approximately -3.8×10^3, that are real and insensitive to perturbation. These are not included in the ϵ-pseudospectra. Since for $c = 3.5$ and $\gamma = 0.022$ the ϵ-pseudospectra of $\mathbf{A}$ are broader than that for $c = 0.035$, we can conclude that the "degree" of non-normality in $\mathbf{A}$ is higher in the former case than in the latter. Another way to verify this is by evaluating the condition number of the eigenvector matrix P of $\mathbf{A}$. In fact, we see that in the former case $\mathrm{cond}(P) = 8.84 \times 10^3$, whereas in the latter $\mathrm{cond}(P) = 3.05$, thus illustrating that $\mathbf{A}$ is close to normal when c is small.

In view of the evidences that $\mathbf{A}$ may become highly non-normal, we conclude that the right way to assure stability of the proposed method is via the pseudoeigenvalue stability criterion. To do this we exploit the fact that the left end of the interval of absolute stability for the fourth-order RK method is known to be approximately 2.78. Using this information we compute the maximum stepsize in the sense of "eigenvalue stability analysis" by the formula

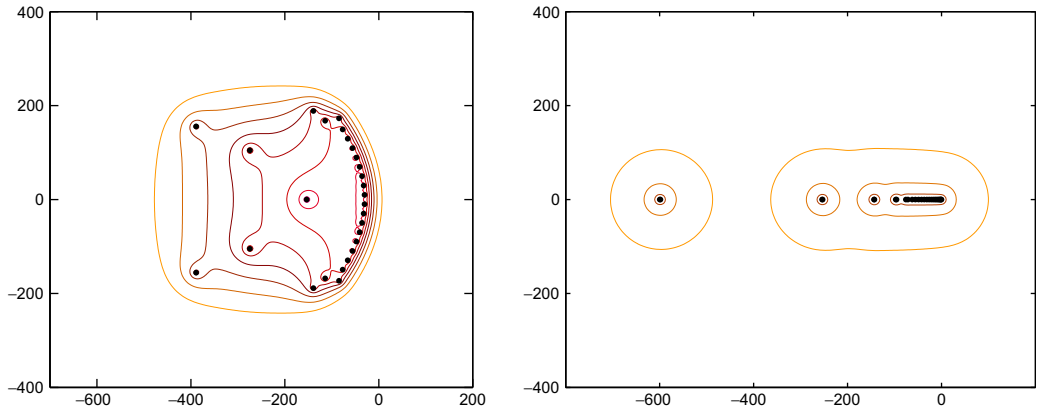

Fig. 2. Left: spectrum and ϵ-pseudospectra of $\mathbf{A}$ for $\epsilon = 10^{k/2}$, $k = -12, -11, \ldots, 2$ with $c = 3.5$ and $\gamma = 0.022$. Right: spectrum and ϵ-pseudospectra of $\mathbf{A}$ for $\epsilon = 10^{k/2}, k = -12, -11, \ldots, 4$ with $c = 0.035$ and $\gamma = 0.022$.

$$\Delta t_{\max} = \frac{2.78}{\rho(\mathbf{A})},$$

where $\rho(\mathbf{A})$ is the spectral radius of $\mathbf{A}$, and then choose the stepsize that guarantees stability by inspecting the ϵ-pseudospectra of $\Delta t\mathbf{A}$ with Δt smaller than $\Delta t_{\max}$. The same procedure was followed in several numerical experiments, two of which we describe in the next section.

5. Numerical examples

We present results of some numerical experiments to illustrate the effectiveness of the proposed method. To this end we choose convection–diffusion equations taken from [7] which are characterized by the fact of having parameter dependent solutions of the form

$$u(x,t) = \exp(\alpha x + \beta t), \quad 0 \leqslant x \leqslant 1, \quad t \geqslant 0,$$

where α, β are adjusted such that the condition $\gamma\alpha^2 - c\alpha - \beta = 0$ is satisfied (see Lemma 1). Initial and boundary conditions are in this case

$$u(x,0) \equiv f(x) = \exp(\alpha x), \quad u(0,t) \equiv g_0(t) = \exp(\beta t), \quad u(1,t) \equiv g_1(t) = \exp(\alpha + \beta t).$$

These equations were solved by the finite difference approach (FDA), implemented as described just after Lemma 1, and by two versions of the pseudospectral method: one based on the Runge–Kutta method (CPS), and the other based on eigenvalue computation (ECPS) as described in (17). Numerical computations were carried out in MATLAB.

Before proceeding, it is worth emphasizing that Salkuyeh's approach cannot work well in these cases as we have seen in Section 2 this approach applies to problems involving constant boundary conditions.

Example 1. Parameters defining problem (1)–(2) and the corresponding solution are

$$c = 3.5, \quad \gamma = 0.022, \quad \alpha = 0.02854797991928, \quad \text{and} \quad \beta = -0.0999$$

This test problem is Example 3 in [7], in which parameter β is taken to be -0.09. This choice of β is not correct: it does not satisfy the necessary condition $\gamma\alpha^2 - c\alpha - \beta = 0$ for $u(x,t) = \exp(\alpha x + \beta t)$ to solve problems (1) and (2) (see Lemma 1).

We now turn our attention to the choice of the stepsize that guarantees stability. Inspection of the spectrum of $\mathbf{A}$ for $n = 20$ reveals that except for a real outlier at -776.2908, the rest of the spectrum comes in complex conjugate pairs and that the spectral radius is determined by the outlier. Maximum stepsize in the sense of eigenvalue stability analysis is thus $\Delta t_{\max} = 0.0036$. Then we analyze the ϵ-pseudospectra of $\mathbf{A}$ and conclude that a reasonable stepsize that assures stable integration is $\Delta t = 0.001$. The appropriateness of this choice fol-

lows from inspecting the ϵ-pseudospectra of $\Delta t\mathbf{A}$ which is displayed in Fig. 3 where we take $\Delta t = 0.003$. Complete inclusion of the ϵ-pseudospectra of $\Delta t\mathbf{A}$ within the region of stability is apparent in this case.

Numerical solutions of the methods at time level $t = 0.1$ for $n = 20$, $\Delta t = 0.001$ and $h = 0.025$ $(m = 40)$, are all displayed in Fig. 4. The time level was chosen to compare the results of our pseudospectral method with those reported in [7]. Unfortunately such a comparison is not done here as our attempts to reproduce the results in [7] were unsuccessful. For this, what we compare in Fig. 4 are the results of our implementation of the finite difference method, which can be verified to be superior than those in [7], with those of the pseudospectral method. The most important conclusion here is the superiority of both versions of the pseudospectral method (ECPS and CPS) over the finite difference method (FDA). Superiority of ECPS over CPS is also notorious in this case. Apart from this, it should be noticed that the results of FDA shown in Fig. 4 (on the left) are consistent with theory as they verify that the truncating error (hence the error itself) is in fact proportional to h^2 (with small constant of proportionality in this case as $\alpha \approx 0$ and $\beta < 0$, see Lemma 2). Fig. 4 (on the right) displays results in the opposite direction: it illustrates that the solution by FDA for $h = 1/55 \approx 0.1818$ $(m = 55)$ deteriorates significantly. The reason is that the eigenvector matrix P of $\mathbf{A}_d$ is severely ill-conditioned as the powers of the quotient $q/r \approx 4.3846$ that enter in the definition of P in (8) are extremely large for $m = 55$, a critical phenomenon that does not occur when $m = 40$ and that was not considered in [7].

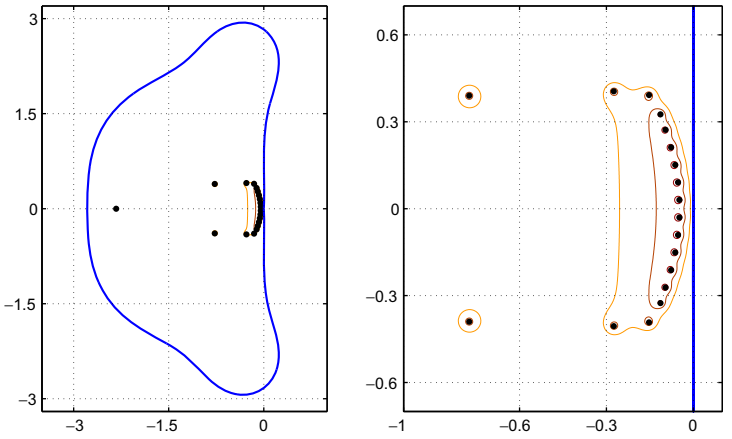

Fig. 3. Left: absolute region of stability for RK-method and ϵ-pseudospectra of matrix $\Delta t\mathbf{A}$ for $\Delta t = 0.003$ and $\epsilon = 10^{-k/2}, k = 4, 5, \ldots, 8$. Right: closer look at the ϵ-pseudospectra.

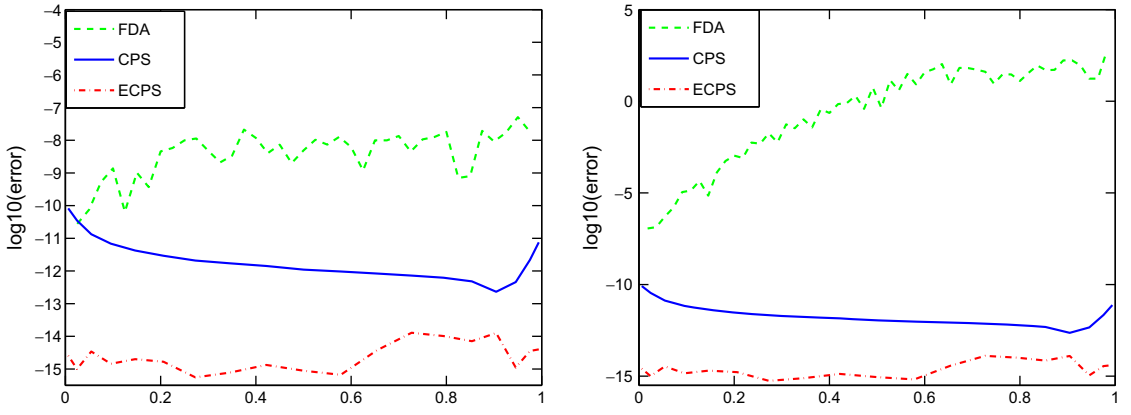

Fig. 4. Left: base 10 logarithm of absolute error of solutions by Chebyshev pseudospectral method and finite differences at $t = 0.1$, for $\Delta t = 0.001$, $n = 20$, and $h = 0.025$ $(m = 40)$. Right: results for $n = 20$, $\Delta t = 0.001$, and $h \approx 0.1818$ $(m = 55)$.

The behavior of CPS for fixed n and decreasing stepsize was also investigated. Results for $n = 20, 30$ and $\Delta t = 0.0001$ are displayed in Fig. 5. What impacts here is the substantial improvement of CPS and the loss of accuracy of solutions by ECPS. The conclusion is that using ECPS may not be always a good idea. The superiority of CPS over ECPS can be explained by saying that eigenvalues were not accurately computed for $n = 30$ due to the influence of the non-normality of matrix $\mathbf{A}$ (as illustrated in the preceding section).

Example 2. Parameters for this example are

$$\alpha = 9, \quad \beta = -0.09, \quad c = 0.1, \quad \gamma = 0.01$$

This test problem is Example 2 in [7]. As in Example 1, the spectral radius of $\mathbf{A}$, for $n = 20$, is determined by the real outlier that in this case occurs at -3.11×10^2. The maximum stepsize according to eigenvalue analysis is $\Delta t_{\max} \approx 0.0089$. Proceeding as before we conclude that $\Delta t = 0.008$ can be a reasonable stepsize, which is supported by Fig. 6 where both the region of absolute stability and the ϵ-pseudospectra of $\Delta t\mathbf{A}$ for $\Delta t = 0.008$ are depicted.

Results of computed numerical solutions for $n = 20$, $\Delta t = 0.001$ and $h = 0.025$ ($m = 40$) are displayed in Fig. 7. Superiority of pseudospectral solutions is once more apparent in this example. $\mathcal{O}(h^2)$ accuracy of FDA is also verified (in this case with constant of proportionality much larger than 1 as $\alpha = 9$, see Lemma 2).

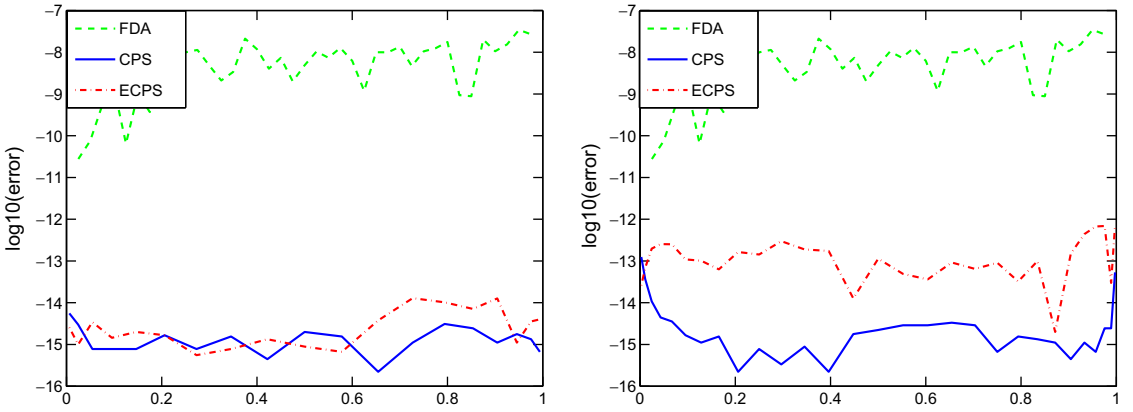

Fig. 5. Left: base 10 logarithm of absolute error of solutions by Chebyshev pseudospectral method and finite differences at $t = 0.1$, for $n = 20$, $\Delta t = 0.0001$ and $h = 0.025$ ($m = 40$). Right: results for $n = 30$, $\Delta t = 0.0001$ and $h \approx 0.025$ ($m = 40$).

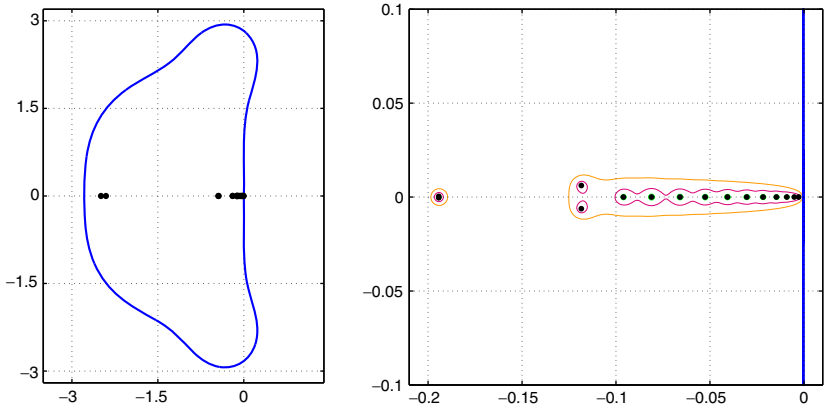

Fig. 6. Left: absolute region of stability for RK-method and ϵ-pseudospectra of matrix $\Delta t\mathbf{A}$ for $\Delta t = 0.008$ and $\epsilon = 10^{k/2}, k = -8, -6, \ldots, -4$. Right: closer look at the ϵ-pseudospectra.

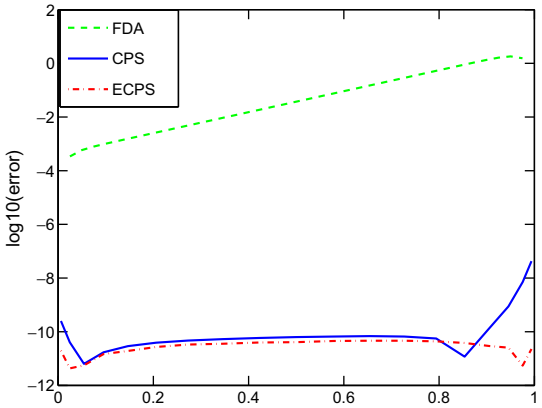

Fig. 7. Base 10 logarithm of absolute error of solutions by Chebyshev pseudospectral method and finite differences at $t = 0.1$, for $n = 20$, $\Delta t = 0.001$ and $h = 0.025$ $(m = 40)$.

6. Concluding remarks

A Chebyshev pseudospectral method for 1D convection–diffusion equations has been proposed and its efficiency illustrated by solving test problems taken from the literature. Stability analysis based on pseudoeigenvalues was also done along with a strategy to determine the timestep that guarantees stability of the proposed method. Further, a review of a finite difference approach by Salkuyeh was carried out, showing that such method does not apply for problems involving time dependent boundary conditions, this being theoretically shown and verified by numerical examples. More study on stability of the semidiscrete system (15) needs to be performed; this and the extension of the method for 2D problems are the subject of ongoing research.

Acknowledgement

This work was supported by CNPq Brasil, Grant 300487/94-O(RN).

References

[1] Chi-Tsong Chen, Linear System Theory and Design, third ed., Oxford University Press, New York, 1999.
[2] C. Canuto, M.Y. Hussaini, A. Quarteroni, T.A. Zang, Spectral Methods in Fluid Dynamics, Springer, New York, 1988.
[3] H.N.A. Ismail, E.M.E. Elbarbary, G.S.E. Salem, Restrictive Taylor's approximation for solving convection–diffusion equation, Appl. Math. Comput. 147 (2004) 355–363.
[4] B. Fornberg, A Practical Guide to Pseudospectral Methods, Cambridge University Press, Cambridge, 1996.
[5] C.D. Meyer, Matrix Analysis and Applied Linear Algebra, SIAM, Philadelphia, 2004.
[6] K.W. Morton, Numerical Solution of Convection–Diffusion Problems, Chapman & Hall, London, 1996.
[7] D. Khojasteh Salkuyeh, On the finite difference approximation to the convection–diffusion equation, Appl. Math. Comput. 179 (2006) 79–86.
[8] S. Reddy, N. Trefethen, Stability analysis of the method of lines, Numer. Math. 62 (1992) 237–267.
[9] G.D. Smith, Numerical Solution of Partial Differential Equations, Oxford University Press, Oxford, 1990.
[10] J.C. Strikwerda, Finite Differences Schemes and Partial Differential Equations, second ed., SIAM, Philadelphia, 2004.
[11] J.W. Thomas, Numerical Partial Differential Equations–Finite Difference Methods, Springer Verlag, New York, 1995.
[12] L.N. Trefethen, Lax stability vs. eigenvalue stability of spectral methods, in: K.W. Morton, M.J. Baines (Eds.), Numerical Methods for Fluid Dynamics III, Clarendon Press, Oxford, 1988.
[13] L.N. Trefethen, Spectral Methods in Matlab, SIAM, Philadelphia, PA, 2000.